Plankton Biol. Ecol. 50 (1): 1–9, 2003

plankton biology & ecology

Light absorption of *Isochrysis galbana* (Prymnesiophyceae) under day-night cycle at high-light irradiance

NOBUAKI OHI, MIWAKO SHINO, YUKI ISHIWATA & SATORU TAGUCHI

Laboratory of Biological Oceanography, Department of Bioengineering, Faculty of Engineering, Soka University, 1–236 Tangi-cho, Hachiouji 192–8577, Japan

Received 11 June 2002; accepted 17 September 2002

Abstract: Diel variation in chl *a* specific absorption coefficients [$a^*(\lambda)$, m^2 (mg chl $a)^{-1}$] was examined to study the effect of pigmentation on $a^*(\lambda)$ of the Prymnesiophyceae *Isochrysis galbana* (Parke) in chemostat culture under 12 h light:12 h dark cycle at 1500 μmol photons $m^{-2} s^{-1}$. Photosynthetic and photoprotective pigment as well as cell density and diameter were also determined at two light regimes every 3 h for 2 days to confirm the periodicity of $a^*(\lambda)$. A distinct diel variation was observed for $a^*(\lambda)$ with maxima toward the end of light periods and minima toward the end of dark periods. The magnitude of diel variation in $a^*(440)$ or $a^*(674)$ was 50% and 24%, respectively. To reconstruct the absorption coefficient, $a_{rec}(\lambda)$, the absorption efficiency factors [$Q_a(674)$] were determined using intracellular chl *a* concentration, cell diameter, and chl *a* specific absorption coefficients after solubilization on Triton X [$a^*_{TX}(\lambda)$]. The contribution of variation in the intracellular chl *a* concentration and cell diameter to the variation in $a^*_{rec}(\lambda)$ was less than one by $a^*_{TX}(\lambda)$. Any changes in $a^*_{TX}(\lambda)$ are due only to changes in the pigmentation. Diel variation in the absorption ratio of photoprotective pigments to chl *a* was observed to be more significant than that for the absorption ratio of other photosynthetic pigments to chl *a*. The diel variations in $a^*(\lambda)$ were primarily caused by changes in pigmentation of photoprotective pigments due to high-irradiance. These results indicated that phytoplankton exhibited 12 h periodic patterns in $a^*(\lambda)$ dependent on high and low irradiance levels.

Key words: absorption, diel cycle, optical properties, pigmentation

Introduction

To understand biogeochemical fluxes (e.g. CO_2) between the atmosphere and the deep ocean, marine primary production is one of the essential processes. It involves a diversity of processes, which vary over a huge range of time and space. Time scales range from minute changes in local physiological rates of phytoplankton to interannual variations at the basin scale. Since satellite ocean color data, for examples the Coastal Zone Color Scanner (CZCS), has been employed to estimates on a global scale (Longhurst et al. 1995; Antoine et al. 1996). Biological models coupled with dynamical model have allowed prediction of primary production at the basin scale (Sarmiento et al. 1993) and investigation of mesoscale dynamics (e.g. Lévy et al. 1998). However there is also a requirement to study high-frequency variability (from hour to day) both in the laboratory and the field in order to complement those studies made on large time and space scales. For example, daily primary production has been estimated from diel variations in optical properties (Stramska & Dickey 1992; Gardner et al. 1993).

Although most observations of the diel variation in optical properties have been focused on the attenuation, scattering and absorption coefficients (Siegel et al. 1989; Dickey et al. 1990; Hamilton et al. 1990; Kroon et al. 1992; Stramska & Dickey 1992; Gardner et al. 1995; DuRand & Olson 1996, 1998), diel variations in the chlorophyll (chl) *a* specific absorption coefficients, $a^*(\lambda)$, have also sometimes been observed (Stramski & Reynolds 1993; Stramski et al. 1995). Ohi et al. (2002) showed recently that the coefficient of variation (CV) of diel variability in $a^*(675)$ for the

Corresponding author: Nobuaki Ohi; e-mail, nooi@edu.t.soka.ac.jp

prymnesiophyceae *Isochrysis galbana* was 7.1% under 75 μmol photons $m^{-2} s^{-1}$ and 9.3% under 500 μmol photons $m^{-2} s^{-1}$ over a 12:12 h light-dark cycle. Variability in $a^*(\lambda)$ can result from a combination of influences on pigmentation that are controlled by photoprotective and photosynthetic pigments (e.g. Sosik & Mitchell 1994) and the pigment packaging effects that vary with cell diameter and intracellular chl *a* content (e.g. Morel & Bricaud 1981). Distinct diel variations in $a^*(\lambda)$ observed for *Isochrysis galbana* with maxima toward the end of dark periods and minima toward the end of light periods under 75 and 500 μmol photons $m^{-2} s^{-1}$ were due to the package effect but not the pigmentation (Ohi et al. 2002). However, diel variation in $a^*(\lambda)$ has not been reported under light irradiance higher than 500 μmol photons $m^{-2} s^{-1}$. Knowledge of the diel variation in $a^*(\lambda)$ is important for determining the optical properties of phytoplankton and could contribute to interpretations of absorption properties and estimates of primary productivity resulting from the high-light irradiance levels that are encountered at the surface layer in temperate and sub-tropical oceans.

The efficiency factor for absorption, $Q_a(\lambda)$, is the ratio of the energy absorbed within a cell to the energy incident on its geometrical cross section. The $Q_a(\lambda)$ and the $a^*(\lambda)$ can be reconstructed from the cell characteristics using the anomalous diffraction approximation (van de Hulst 1957). Based solely on the intracellular chl *a* concentration, cell diameter and the unpackaged chl *a* specific absorption coefficients after solubilization in Triton X, the reconstruction of $a^*(\lambda)$ proposed in this study, via the Q_a factors, may provide a better opportunity to determine the relative significance of package effect and pigmentation than the other methods (Bricaud et al. 1999). Such reconstruction can be used to determine whether the observed absorption properties are thoroughly consistent with reconstructed $a^*(\lambda)$ and predictable from cell characteristics. This reconstruction is also aimed at determining the respective contributions of factors responsible for changes in the absorption properties of phytoplankton cells.

In the experiments reported here on diel variations in $a^*(\lambda)$ of a phytoplankton species, we chose the prymnesiophyceae *Isochrysis galbana* because there is a pronounced diel pattern in cell diameter, when cell division is tightly phased to the light: dark cycle (e.g. Ohi et al. 2002). The aims of this paper are therefore (1) to describe the diel variability in light absorption properties of *Isochrysis galbana* under high-light conditions at 1500 μmol photons $m^{-2} s^{-1}$; (2) to differentiate between package effects and pigmentation effects on the diel variation in $a^*(\lambda)$; (3) to reconstruct the $a^*(\lambda)$ spectra from the cell characteristics and to determine how the package effect and pigmentation effect contribute to the diel variations in $a^*(\lambda)$. A list of notations is provided in Table 1.

Table 1. Definition of mathematical symbols and associated units.

Symbol	Definition	Units
λ	Wavelength	nm
OD(λ)	Optical density of sample in suspention	—
[Chl *a*]	Chl *a* concentration	mg m^{-3}
$a(\lambda)$	Absorption coefficient of phytoplankton	m^{-1}
$a_{TX}(\lambda)$	Absorption coefficient after solubilization in Triton X-100	m^{-1}
$a_{rec}(\lambda)$	Reconstructed absorption coefficient of phytoplankton	m^{-1}
$a_{total}(\lambda)$	Absorption coefficient of total pigments $=\sum a_{pig}$	m^{-1}
$a_{pig}(\lambda)$	Absorption coefficient of pigment *p*	m^{-1}
$a_{Chl\,a}(\lambda)$	Absorption coefficient of chl *a*	m^{-1}
$a_{Chl\,c}(\lambda)$	Absorption coefficient of chl c_{1+2}	m^{-1}
$a_{Fuco}(\lambda)$	Absorption coefficient of fucoxanthin	m^{-1}
$a_{DD+DT}(\lambda)$	Absorption coefficient of diadinoxanthin plus diatoxanthin	m^{-1}
$a_{\beta\text{-carot}}(\lambda)$	Absorption coefficient of β,β-carotene	m^{-1}
$a^*_{sol,p}(\lambda)$	*In vivo* weight-specific absorption coefficient of pigment *p*	m^2 mg^{-1}
$a^*(\lambda)$	Chl *a* specific absorption coefficient	m^2 mg^{-1}
$a^*_{TX}(\lambda)$	Chl *a* specific absorption coefficient after solubilization in Triton X-100	m^2 mg^{-1}
$a^*_{rec}(\lambda)$	Reconstructed chl *a* specific absorption coefficient	m^2 mg^{-1}
$a_{cm}(\lambda)$	Absorption coefficient of the cell material	m^{-1}
N	Number of cells	cells
V	Volume of the suspension	m^{-3}
d	Mean cell diameter of the population	m
$Q_a(\lambda)$	Efficiency factor for absorption	—
ρ'	Optical thickness along the particle diameter	—
$c_{i,p}$	Intracellular concentration of pigment *p*	kg m^{-3}
$c_{Chl\,a}$	Intracellular chl *a* concentration	kg m^{-3}

Materials and Methods

Culturing procedure and sampling

Prymnesiophyceae *Isochrysis galbana* Parke (NEPCC 633) were obtained from The North East Pacific Culture Collection (NEPCC) at the University of British Columbia, Canada. *I. galbana* was grown at 25°C in 1 L culture in seawater enriched with f/2 medium (Guillard & Ryther 1962). Steady state growth rates were established at 1.72 d^{-1} at 1500 μmol photons $m^{-2} s^{-1}$, which was determined by a Biospherical Instrument QSL-100 quantum scalar irradiance meter. Light was provided in a 12 h light and 12 h dark cycle by cool-white fluorescent tubes. Careful aseptic techniques were used to minimize bacterial contamination in the maintenance and growth of the culture. The culture was operated in a continuous turbidostat for two weeks with the dilution rate dictated by the growth rate of cells. Cell numbers were determined twice a day to confirm a synchronized and steady growth. At each sampling, fresh media were added via a peristaltic pump to maintain relatively constant cell density within the optically thin suspension. Cells were kept in suspension by a combination of continuous stirring and bubbling sterile air. Separate duplicate samples were collected for the determination of absorption coefficient and pigments every 3 h for 51 h. These samples were filtered onto 25 mm GF/F glass fiber filters (Whatman) under pressure lower than 120 mmHg.

Cell number and diameter

Samples were preserved by adding 10% neutralized formaldehyde to obtain a 2% final concentration and stored in the dark at 4°C. We determined that such treatment for this species induced only minor changes in cell diameter (<5%). Cell numbers were measured under a microscope with a haemacytometer (Bright-Line, Erma Inc.). Spherical cell diameters of 75 cells were measured under the microscope with an ocular ruler at 1000×magnification. The average cell volume was calculated from the average cell diameter, d, under the assumption that all cells were spherical.

Absorption coefficients

Optical densities, OD(λ), of suspensions were determined with a Shimadzu UV–2450 spectrophotometer equipped with an integrating sphere, with reference to a filtrate of the suspension (Whatman GF/F glass fiber filter). The integrating sphere neutralizes wavelength-dependent scattering which causes errors with conventional methodology (Johnsen et al. 1994). Absorption coefficients, $a(\lambda)$, were obtained as:

$$a(\lambda)=2.3\ \mathrm{OD}(\lambda)/r \qquad (1)$$

where r (=0.01 m) is the pathlength of the cuvette. Spectral values of the absorption coefficient were recorded every 1 nm from 350 to 750 nm. All spectra were set to zero at 750 nm to minimize differences between sample and reference, assuming lack of absorption by particles at 750 nm. The chl a specific absorption coefficients, $a^*(\lambda)$, were obtained from the absorption coefficients, $a(\lambda)$, according to:

$$a^*(\lambda)=a(\lambda)/[\mathrm{Chl}\ a] \qquad (2)$$

where [Chl a] is chlorophyll a concentration.

To differentiate between package and pigmentation effects on the diel variation in $a^*(\lambda)$, cells were solubilized in the detergent Triton X-100 at a final concentration of 0.5% (in volume) with subsequent sonication as recommended by Berner et al. (1989). The Triton extracts were centrifuged, and spectral absorption, $a_{TX}(\lambda)$, was determined on these solubilized cells with 0.5% Triton X-100 in filtered seawater as a reference. These chl a specific absorption coefficients for samples solubilized in Triton X-100, $a^*_{TX}(\lambda)$, were calculated as described for $a^*(\lambda)$. Because the Triton X removes the effect of packaging pigments in the cells and chloroplasts, any changes in $a^*_{TX}(\lambda)$ are due only to changes in the pigmentation. The Triton X method involves spectral shifts in the wavelengths of peak absorption when compared to *in vivo* absorption. In fact, we have observed shifts toward shorter wavelengths by 1 nm at the blue peak and 8 nm at the red peak. To compensate for these shifts when using $a^*_{TX}(\lambda)$ in calculations or comparison with $a^*(\lambda)$, we have shifted the spectra by 1 nm for wavelengths 350–557 nm and 8 nm for 551–750 nm. The region between 551 and 557 nm was repeated to prevent introducing a gap in the spectra; values were relatively low and uniform at these wavelengths, so this treatment did not distort the spectra.

Pigments

The filtered samples were sonificated for 10 min in 10 ml of 90% acetone, and extracted for 24 h at 4°C. Following extraction, pigment samples were centrifuged for 5 min to remove cellular debris. Pigment analysis was carried out by HPLC (System Gold, Beckman) using the solvent gradient system described by Head & Horne (1993). Identified pigments were chl c_{1+2}, fucoxanthin, diadinoxanthin, diatoxanthin, chl a and β,β-carotene. Integrated peak areas were quantified with external standards obtained from the International Agency for ^{14}C Determination.

Reconstruction of absorption efficiency factors from cell characteristics and package effect

Cells are assumed to be spherical and homogeneous with respect to the refractive index when the anomalous diffraction approximation is made (van de Hulst 1957). The reconstructed chl a specific absorption coefficients, $a^*_{rec}(\lambda)$, can be estimated by dividing the reconstructed absorption coefficients, $a_{rec}(\lambda)$, by [Chl a]. The $a_{rec}(\lambda)$ can be estimated using the number of cells, N, in a volume of the suspension, V, the efficiency factors for absorption, $Q_a(\lambda)$ and the geo-

metric cross-section determined by spherical cell diameter, d (Morel & Bricaud 1981):

$$a_{rec}(\lambda)=N/V \cdot Q_a(\lambda) \cdot (\pi/4)d^2. \quad (3)$$

The $Q_a(\lambda)$ for a single cell, that is, the ratio of absorbed to energy incident on the geometrical cross section of the cell, can be estimated as:

$$Q_a(\lambda)=1+2\exp[-\rho'(\lambda)]/\rho'(\lambda) +2\{\exp[-\rho'(\lambda)]-1\}/\rho'(\lambda)^2 \quad (4)$$

in which $\rho'(\lambda)=a_{cm}(\lambda) \cdot d$. The $a_{cm}(\lambda)$ coefficients were here computed from the intracellular chl a concentration, $c_{Chl\,a}$, and the $a^*_{TX}(\lambda)$ (Sosik & Mitchell 1991) according to:

$$a_{cm}(\lambda)=a^*_{TX}(\lambda) \cdot c_{Chl\,a} \quad (5)$$

where $c_{Chl\,a}$ is the ratio of [Chl a] to the product of cell volume and cell density:

$$c_{Chl\,a}=[\text{Chl } a]/[(\pi/6)d^3 \cdot N/V]. \quad (6)$$

The intracellular concentrations of various pigments p, $c_{i,p}$, were computed from each pigment, p, using equation (6).

Contribution of pigmentation to $a^*(\lambda)$

We examined pigmentation, which affects the magnitude of diel variation in $a^*(440)$. The contribution of each pigment to the variation in $a^*(\lambda)$ is equal to the product of the intracellular concentrations of various pigments, $c_{i,p}$, and the *in vivo* pigment specific absorption coefficients. *In vivo* absorption coefficients of various pigment, $a_{pig}(\lambda)$, were related to *in vivo* absorption coefficients of total pigments, $a_{total}(\lambda)$, according to:

$$a_{pig}(\lambda)/a_{total}(\lambda)=c_{i,p} \cdot a^*_{sol,p}(\lambda)/\sum_{i=1}^{n} c_{i,p} \cdot a^*_{sol,p}(\lambda) \quad (7)$$

where the value for the *in vivo* weight-specific absorption coefficient of pigment p, $a^*_{sol,p}(\lambda)$, was the *in vivo* weight-specific absorption coefficient proposed by Fujiki and Taguchi (2001). This technique does not take into account pigment packaging effects, but resolves issues regarding spectral shape and molar *in vivo* absorption coefficients. Despite these problems, the method allowed us to assess the relative importance of pigmentation to diel variation in $a^*(\lambda)$.

Mathematical and statistical analysis

The periodicity of the rhythm was analyzed by a modified function of the Cosinor function (Halberg et al. 1978; Kieding et al. 1984) as follows:

$$Y=A+Bt+C\sin[(t+e)\pi/(12+f)] +G\cos[(t+e)\pi/(12+f)] \quad (8)$$

where Y is an estimate of a circadian variable [e.g. $a^*(\lambda)$, cell diameter, etc.], A is the average of the circadian variable, B is gradient, t is time in hours, e is the difference between the 12 h cycle and the length of a cycle, and (12+f) is the length of one cycle. C is the amplitude of the sinor function and G is the amplitude of the cosinor function, thus the amplitude of the rhythm is calculated as $(C^2+G^2)^{1/2}$. A nonlinear least squares regression analysis was used to test the degree of fitness of the estimated value to the observed value.

The magnitude of diel variation (%) for each variable was calculated as follows:

$$\text{The magnitude of diel variation}=|\text{Max}-\text{Min}|/\text{Min}\times 100 \quad (9)$$

where Max is $A+(C^2+G^2)^{1/2}$ and Min is $A-(C^2+G^2)^{1/2}$.

Results

The $a^*(\lambda)$ spectra throughout a diel cycle exhibited absorption bands corresponding to chl a at around 440 and 674 nm, bands corresponding to accessory pigments at around 460 and 490 nm, and spectral regions of relatively weak absorption between 586 and 635 nm (Fig. 1). When the Cosinor function was fitted to the parameter data, the results (Table 2) clearly show that the difference is insignifi-

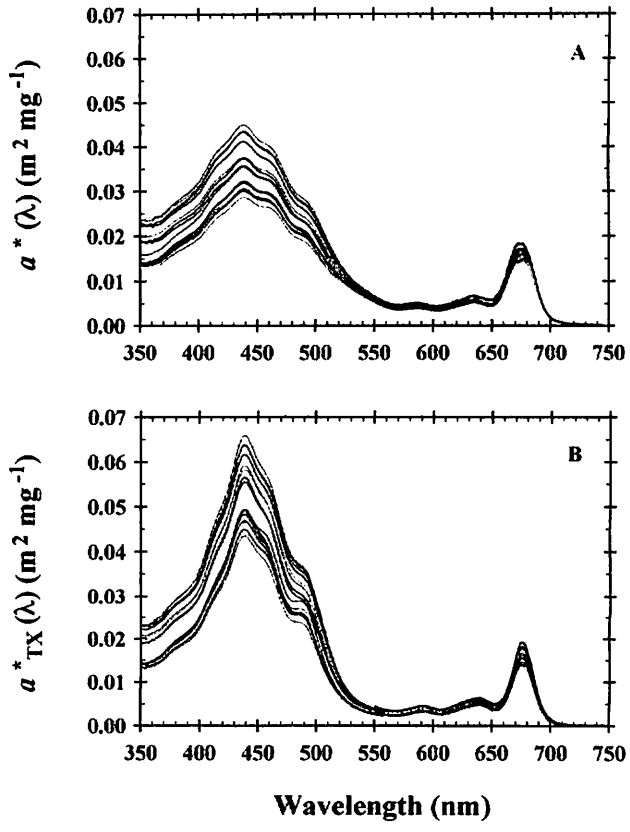

Fig. 1. Diel variation in spectral values of the chl a specific absorption coefficients [$a^*(\lambda)$] (A) and $a^*(\lambda)$ after solubilization in 0.5% Triton X-100 [$a^*_{TX}(\lambda)$] (B) for *Isochrysis galbana*. Each panel includes 18 spectra determined throughout the experiments.

Table 2. Values for chl *a* concentration [Chl *a*], cell density [N/V], chl *a* specific absorption coefficient [$a^*(\lambda)$], $a^*(\lambda)$ after solubilization in 0.5% Triton X-100 [$a^*_{TX}(\lambda)$], reconstructed $a^*(\lambda)$ [$a^*_{rec}(\lambda)$] and efficiency factor for absorption [$Q_a(\lambda)$] at 440 and 674 nm, mean cell diameter (d) and pigment ratios (Fuco: fucoxanthin, DD: diadinoxanthin, DT: diatoxanthin, β,β-carotene: β-carot) and reconstructed absorption ratios of pigments to total pigment at 440 nm for *Isochrysis galbana*. The minimal and maximal values and magnitude of diel variation (%) of the parameters estimated using a Cosinor fit to the data as in equation (8) are indicated. Minus signs indicate decrease during the light periods.

	Max.	Min.	%
[Chl *a*] (mg m^{-3})	1593	1125	−41.6
N/V (10^{-12} cells m^{-3})	6.0	3.9	−55.9
$a^*(440)$ (m^2 mg^{-1})	0.0452	0.0300	50.3
$a^*(674)$ (m^2 mg^{-1})	0.0187	0.0157	19.3
$a^*_{TX}(440)$ (m^2 mg^{-1})	0.0652	0.0454	43.6
$a^*_{TX}(674)$ (m^2 mg^{-1})	0.0192	0.0146	31.0
$a^*_{rec}(440)$ (m^2 mg^{-1})	0.0342	0.0450	17.6
$a^*_{rec}(674)$ (m^2 mg^{-1})	0.0157	0.0127	23.9
$Q_a(440)$	0.72	0.59	23.3
$Q_a(674)$	0.33	0.25	28.9
d (μm)	4.2	4.0	5.6
Chl c_{1-2}/chl *a*	0.10	0.098	−5.3
Fuco/chl *a*	0.35	0.25	−37.0
DD+DT/chl *a*	0.27	0.17	62.1
β-carot/chl *a*	0.049	0.040	24.9
$a_{Chl\ a}/a_{Total}$	0.57	0.53	−7.7
$a_{Chl\ c}/a_{Total}$	0.11	0.095	−12.9
a_{Fuco}/a_{Total}	0.14	0.098	−39.7
a_{DD+DT}/a_{Total}	0.22	0.15	49.8
$a_{\beta\text{-carot}}/a_{Total}$	0.049	0.042	15.8

cant. The significant 1 : 1 linear relationship between all measured data in the present study (Table 2) and the data estimated by equation (8) indicates distinct diel variation. Distinct diel variations in measured $a^*(\lambda)$ were observed for the red absorption maximum at 674 nm and the blue absorption maximum at 440 nm with maxima toward the end of light periods and minima toward the end of dark periods ($p<0.001$) (Fig. 2). The magnitude of diel variation in $a^*(\lambda)$ was 19% at 674 nm and 50% at 440 nm (Table 2).

In detergent solubilized samples, the absorption peak shifted toward shorter wavelengths of 1 nm at the blue peak and 8 nm at the red peak. The spectral values of $a^*_{TX}(\lambda)$ have been presented following adjustment (Fig. 1). Distinct diel variations in $a^*_{TX}(\lambda)$ at 674 and 440 nm were also present with maxima toward the end of light periods and minima toward the end of dark periods ($p<0.001$) (Fig. 2). The magnitude of diel variation in $a^*_{TX}(\lambda)$ was 31% at 674 nm and 44% at 440 nm (Table 2).

Distinct diel variations were observed for [Chl *a*] and N/V with maxima toward the end of dark periods and minima toward the end of light periods ($p<0.001$). The magnitude of diel variation was 42% for [Chl *a*] and 56% for N/V, respectively (Table 2). The d exhibited a distinct diel variation with maxima toward the end of light periods and minima toward the end of dark periods ($p<0.001$) (Fig. 3). The magnitude of diel variation in d was 5.6% (Table 2). Distinct diel variations were not obtained for $c_{Chl\ a}$ ($p>0.05$). The coefficient of variation throughout a diel cycle was 5.7% for $c_{Chl\ a}$.

The predominant pigments found in this study are in agreement with the previous findings of Zapata & Garrido (1997). Distinct diel variations were observed for the fucoxanthin/chl *a* and chl c_{1-2}/chl *a* ratios with maxima toward the end of light periods and minima toward the end of dark periods ($p<0.001$) (Fig. 3). Distinct diel variations were also obtained for the (diadinoxanthin plus diatoxanthin)/chl *a* and β,β-carotene/chl *a* ratios with a 12 h shift in the periodicity ($p<0.001$) (Fig. 3). The increase in $a^*(440)$ or $a^*_{TX}(440)$ during the light periods (Fig. 2) was parallel to an increase in (diadinoxanthin plus diatoxanthin)/chl *a* ratio by 62% and β,β-carotene/chl *a* ratio by 25%, and a decrease in fucoxanthin/chl *a* and chl c_{1-2}/chl *a* ratios of 37% and 5.3%, respectively (Table 2).

The relative importance to total pigment absorption of reconstructed absorption due to each pigment was examined. The reconstructed absorption of chl *a*, $a_{Chl\ a}(440)$, contributed to the reconstructed absorption of total pigment, $a_{Total}(440)$, by 53–57% throughout a diel cycle. The relative importance of the various pigments to $a_{Total}(440)$ was followed by diadinoxanthin plus diatoxanthin, fucoxanthin, chl c_{1-2} and β,β-carotene in order. Distinct diel variations were observed for the ratios of $a_{Chl\ a}$ or a_{Fuco} to a_{Total} at 440 nm with maxima toward the end of light periods and minima toward the end of dark periods ($p< 0.001$) (Fig. 6).

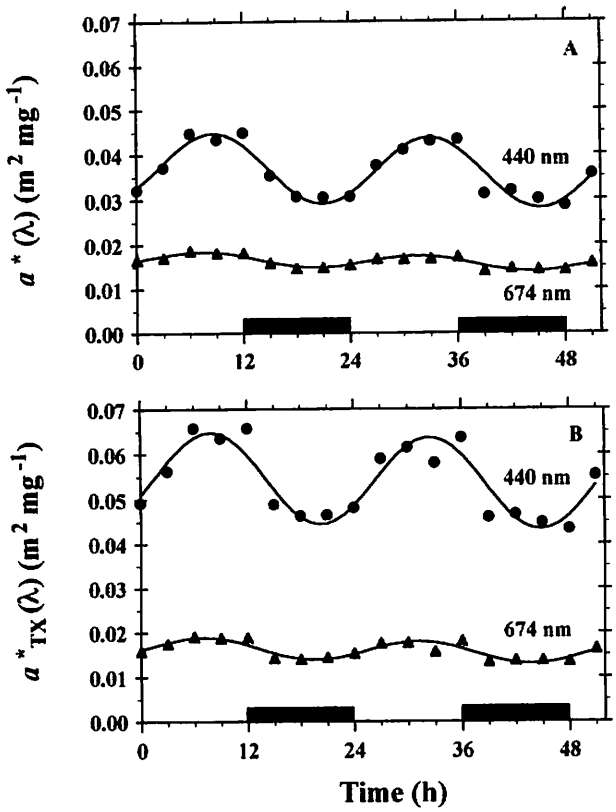

Fig. 2. Diel variations in the chl *a* specific absorption coefficients [$a^*(\lambda)$] (A) and $a^*(\lambda)$ after solubilization in 0.5% Triton X-100 [$a^*_{TX}(\lambda)$] (B) at 440 (●) and 674 (▲) nm for *Isochrysis galbana*. The curve represents a Cosinor fit. Dark bars indicate dark periods.

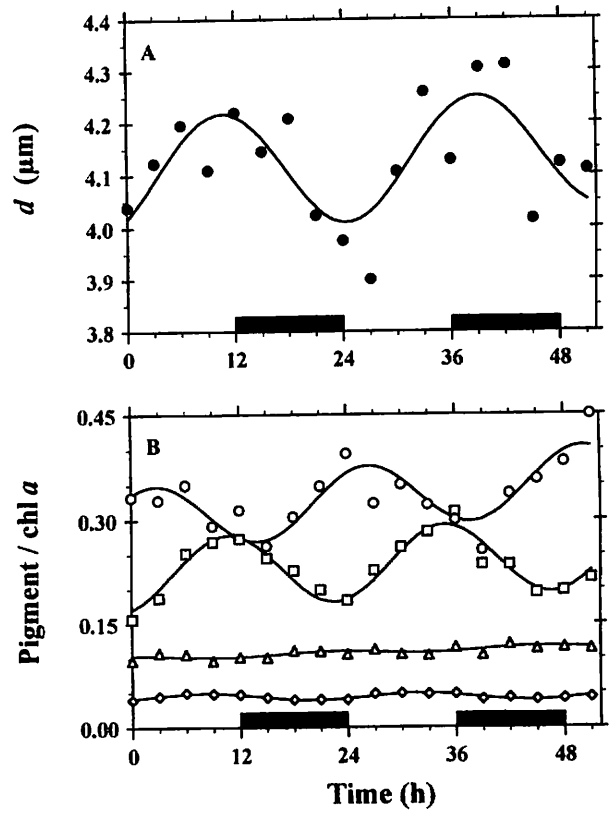

Fig. 3. Diel variations in the cell diameter (*d*) (A) and the ratios of pigments to chl *a* (B) for *Isochrysis galbana*. Symbols indicate the ratios of fucoxanthin (○), diadinoxanthin plus diatoxanthin (□), chl c_{1+2}(△) and β,β-carotene (◇) to chl *a*. The curve represents a Cosinor fit. Dark bars indicate dark periods.

In contrast, distinct diel variations were observed for the ratios of a_{DD+DT} or $a_{\beta\text{-carot}}$ to a_{Total} at 440 nm with a 12 h shift in the periodicity ($p<0.001$) (Fig. 6). The increase in $a^*(\lambda)$ at 440 nm during the light periods was parallel to increase in the a_{DD+DT}/a_{Total} ratio by 50% and the $a_{\beta\text{-carot}}/a_{Total}$ ratio by 16% for photoprotective pigments, with a decrease in $a_{Chl\ a}/a_{Total}$ ratio by 7.7%, $a_{Chl\ c}/a_{Total}$ ratio by 13% and a_{Fuco}/a_{Total} ratio by 40%, respectively (Table 2).

Discussion

Shifting in the phase of diel cycle of $a^*(\lambda)$

The diel pattern in $a^*(\lambda)$ was characterized by maxima toward the end of light periods and minima toward the end of dark periods at 1500 μmol photons m^{-2} s^{-1}. However, Ohi et al. (2002) have reported a contrary diel pattern in $a^*(\lambda)$ for the same species *I. galbana* with maxima toward the end of dark periods and minima toward the end of light periods at lower irradiance (500 μmol photons m^{-2} s^{-1}) than that in the present study. The results presented here and published previously provide strong evidence that the same species of phytoplankton exhibits 12 h shifted diel patterns in $a^*(\lambda)$ depending on whether irradiance levels are high or low. Reverse shifted diel patterns in the size-fractionated chl *a* specific absorption coefficients of surface picophytoplankton, $a^*_{pico}(\lambda)$, have also been observed to depend on high or low irradiance levels in the western subarctic Pacific (Ohi et al.; in preparation). These reverse shifted diel patterns in $a^*_{pico}(\lambda)$ were primarily caused by contrary changes in intracellular chlorophyll *a* concentration due to photoadaptation to high- and low-irradiance levels, although there was some influence of pigmentation in the blue to red ratio [$a^*_{pico}(443)/a^*_{pico}(675)$] under high-light irradiance levels.

Reconstructed absorption coefficients and efficiency factors for absorption

Distinct diel variations in reconstructed $a^*_{rec}(\lambda)$ at 440 and 674 nm were also observed with maxima toward the end of light periods and minima toward the end of dark periods ($p<0.001$) (Fig. 4). Relationships between diel variation in experimental $a^*(\lambda)$ and diel variation in reconstructed $a^*_{rec}(\lambda)$ are significantly correlated (r=0.76, $p<$ 0.001 at 440 nm; r=0.92, $p<0.001$ at 674 nm), but the slopes of the regression lines are 0.36 at 440 nm and 0.91 at 674 nm. The reconstructed values are lower than the mea-

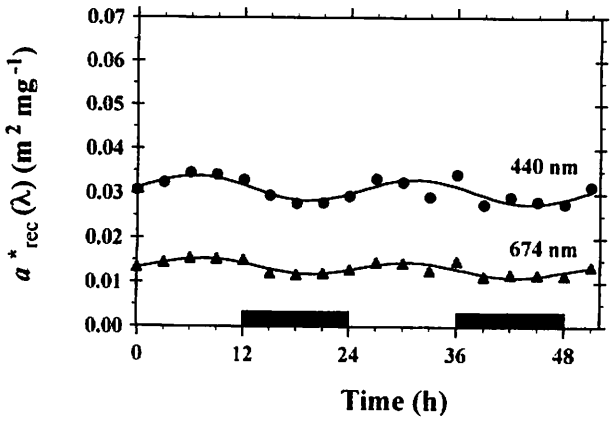

Fig. 4. Diel variations of the reconstructed chl *a* specific absorption coefficients [$a^*_{rec}(\lambda)$] at 440 (●) and 674 (▲) nm for *Isochrysis galbana*. The curve represents a Cosinor fit. Dark bars indicate dark periods.

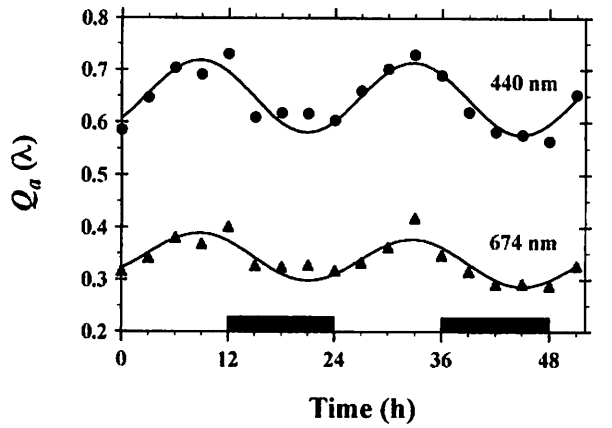

Fig. 5. Diel variations in the reconstructed values of the efficiency factors [$Q_a(\lambda)$] at 440 (●) and 674 (▲) nm for *Isochrysis galbana*. The curve represents a Cosinor fit. Dark bars indicate dark periods.

sured values by on average 64% at 440 nm and 9% at 674 nm although the reconstruction is fairly satisfactory at 674 nm. These differences may originate from various sources: (1) experimental errors in the estimation of N/V, $c_{Chl\,a}$ and d used for the theoretical computations; (2) experimental errors in absorption measurement and (3) deviations from the assumptions [equation (5)] introduced in these computations (e.g. Bricaud et al. 1999; Moisan & Mitchell 1999). Therefore, the magnitude of diel variation in $a^*_{rec}(\lambda)$ is underestimated and may not provide a satisfactory quantitative estimate. In spite of these differences and various uncertainties, the diel patterns in $a^*(\lambda)$ corresponded to the diel pattern in $a^*_{rec}(\lambda)$. Therefore, this allows us to examine how the various parameters contribute to the $a^*(\lambda)$, or equivalently $Q_a(\lambda)$, variations over their diel cycle.

Distinct diel variations were observed for the $Q_a(\lambda)$ at 440 and 674 nm with maxima toward the end of light periods and minima toward the end of dark periods ($p<0.001$) (Fig. 5). Diel variation in $Q_a(\lambda)$ was estimated from the

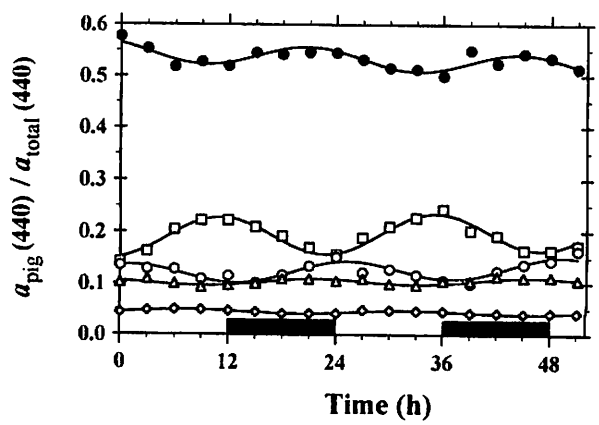

Fig. 6. Diel variations in the reconstructed absorption ratios of pigments to total pigment [$a_{pig}(440)/a_{total}(440)$] for *Isochrysis galbana*. Symbols indicate the chl *a* (●), fucoxanthin (○), diadinoxanthin plus diatoxanthin (□), chl c_{1+2} (△) and β,β-carotene (◇). The curve represents a Cosinor fit. Dark bars indicate dark periods.

product of the intracellular chl *a* concentration, $c_{Chl\,a}$, the cell diameter, d and $a^*_{TX}(\lambda)$ [Eqs. (4), (5), (6)]. The $c_{Chl\,a} \cdot d$ could be related to pigment packaging, which alters the $a^*(\lambda)$ (Ciotti et al. 1999). However, distinct diel variations were not obtained for $c_{Chl\,a} \cdot d$ and $c_{Chl\,a}$ ($p>0.05$). Distinct diel variations held for $a^*_{TX}(\lambda)$ at 674 and 440 nm and d with maxima toward the end of light periods and minima toward the end of dark periods ($p<0.001$) (Figs. 2 and 3). Contribution of variations in the intracellular chl *a* concentrations and cell diameter to the variation of $a^*_{rec}(\lambda)$ was less than one by $a^*_{TX}(\lambda)$ (Table 2). Any changes in $a^*_{TX}(\lambda)$ are due only to changes in the pigmentation as described above. Therefore, the diel variation in $Q_a(\lambda)$ was primarily due to diel variation in the pigmentation.

Contribution of pigmentation to diel variation in $a^*(\lambda)$

We examined the contribution of pigmentation and its effect on the diel variation in $a^*(440)$. Increase in pigmentation due to changes in the relative proportions of chl *a* and accessory pigments during the light periods resulted from an increase in photoprotective pigments, especially the diadinoxanthin plus diatoxanthin, to chl *a* ratio (Fig. 3). Similar results under a light: dark cycle at high-light irradiance have been observed for the photosynthetic and photoprotective pigment to chl *a* ratio (e.g. Kohata & Watanabe 1989) and diadinoxanthin plus diatoxanthin to chl *a* ratio (e.g. Demers et al. 1991). The increase in $a^*(440)$ during the light periods was due mainly to both an increase in $a_{DD+DT}(440)$ and a decrease in $a_{Chl\,a}(440)$ during the light periods over the diel cycle. The increase in $a^*(440)$ during the light periods seemed to directly affect the amount of absorbed light energy.

Implication for field observations

The results in this study provide strong evidence that the $a^*(\lambda)$ can increase during the day under a diel cycle in the surface layer of the ocean. Diel patterns in photosynthetic- and photoprotective-pigments due to photoadaptation were the primary cause of the diel pattern in $a^*(\lambda)$ under high light conditions, although diel variation in package effect also contributed. Because the diel patterns in pigmentation of *I. galbana* were similar to other phytoplankton species at high irradiance levels (Kohata & Watanabe 1989), these results seem to be important for interpreting diel variations in oceanic surface optical properties. The results presented here and published previously (Ohi et al. 2002) suggest that phytoplankton can exhibit 12 h shifted diel patterns in $a^*(\lambda)$ from the surface layer to deep layers in the euphotic zone. The measurement of light-depth dependent optical properties presents a new challenge for assessing the impact of this phenomenon on the procedures for estimating phytoplankton biomass and production.

Literature Cited

Antoine, D., J. M. André & A. Morel 1996. Oceanic primary production, 2, Estimation at global scale from satellite (coastal zone color scanner) chlorophyll. *Global Biogeochem. Cycles* **10**: 57–69.

Berner, T., Z. Dubinsky, K. Wyman & P. G. Falkowski 1989. Photoadaptation and the "package" effect in *Dunaliella tertiolecta* (Chlorophyceae). *J. Phycol.* **25**: 70–78.

Bricaud, A., K. Allali, A. Morel, D. Marie, M. J. W. Veldhuis, F. Partensky & D. Vaulot 1999. Divinyl chlorophyll *a*-specific absorption coefficients and absorption efficiency factors for *Prochlorococcus marinus*: kinetics of photoacclimation. *Mar. Ecol. Prog. Ser.* **188**: 21–32.

Ciotti, M., J. J. Cullen & M. R. Lewis 1999. A semi-analytical model of the influence of phytoplankton community structure on the relationship between light attenuation and ocean color. *J. Geophys. Res.* **104**: 1559–1578.

Demers, S., S. Roy, R. Gagnon & C. Vignault 1991. Rapid light-induced changes in cell fluorescence and in xanthophyll-cycle pigments of *Alexandrium excavatum* (Dinophyceae) and *Thalassiosira pseudonana* (Bacillariophyceae): a photo-protection mechanism. *Mar. Ecol. Prog. Ser.* **76**: 185–193.

Dickey, T., T. Granata, M. Hamilton, J. Wiggert, J. Marra, C. Langdon & D. A. Siegel 1990. Time series observations of bio-optical properties in the upper layer of the Sargasso Sea. *Proc. Int. Soc. Opt. Eng.* Ocean Optics X. **1302**: 202–213.

DuRand, M. D. & R. J. Olson 1996. Contributions of phytoplankton light scattering and cell concentration changes to diel variations in beam attenuation in the equatorial Pacific from flow cytometric measurements of pico-, ultra- and nanoplankton. *Deep-Sea Res. II.* **43**: 891–906.

DuRand, M. D. & R. J. Olson 1998. Diel patterns in optical properties of the chlorophyte *Nannochloris* sp.: Relating individual-cell to bulk measurements. *Limnol. Oceanogr.* **43**: 1107–1118.

Fujiki, T. & S. Taguchi 2001. Relationship between light absorption and the xanthophyll-cycle pigments in marine diatoms. *Plankton Biol. Ecol.* **48**: 96–103.

Gardner, W. D., I. D. Walsh & M. J. Richardson 1993. Biophysical forcing of particle production and distribution during a spring bloom in the North Atlantic. *Deep-Sea Res. II.* **40**: 171–195.

Gardner, W. D., S. P. Chung, M. J. Richardson & I. D. Walsh 1995. The oceanic mixed-layer pump. *Deep-Sea Res.* **42**: 757–775.

Guillard, R. R. L. & J. H. Ryther 1962. Studies of marine planktonic diatoms. I. *Cyclotella nana* Hustedt and *Detonula confervacea* (Cleve). *Gran. Can. J. Microbiol.* **8**: 229–239.

Halberg, F., E. Haus & L. E. Scheving 1978. Sampling of biologic rhythms, chronocytokinetics and experimental oncology. p. 175–190. In *Biomathematics and Cell Kinetics* (ed. Valleron, A-J. & P. D. M. Macdonald). New York. (Elsevier Biomedical Press)

Hamilton, M., T. C. Granata, T. D. Dickey, J. D. Wiggert, D. A. Siegel, J. Marra & C. Langdon 1990. Diel variations of bio-optical properties in the Sargasso Sea. *Proc. Int. Soc. Opt. Eng.* Ocean Optics X. **1302**: 214–224.

Head, E. J. H. & P. W. Horne 1993. Pigment transformation and vertical flux in an area of convergence in the North Atlantic. *Deep-Sea Res. II.* **40**: 329–346.

Johnsen, G., N. B. Nelson, R. V. M. Jovine & B. B. Prézelin 1994. Chromoprotein- and pigment-dependent modeling of spectral light absorption in two dinoflagellates, *Prorocentrum minimum* and *Heterocapsa pygmaea*. *Mar. Ecol. Prog. Ser.* **114**: 245–258.

Kieding, N., N. Rudolph & U. Møller 1984. Diurnal variation in influx and transition intensities in the S phase of hamster cheek pouch epithelium cells, p. 135–159. In *Cell Cycle Clocks* (ed. Edmunds, L. Jr.). New York. (Marcel Dekker, Inc.)

Kohata , K & M. Watanabe 1989. Diel changes in the composition of photosynthetic pigments and cellular carbon and nitrogen in *Pyramimonas parkeae* (Prasinophyceae). *J. Phycol.* **25**: 377–385.

Kroon, B. M. A., M. Latasa, B. W. Ibelings & L. R. Mur 1992. The effect of dynamic light regimes on *Chlorella*. I. Pigments and cross sections. *Hydrobiologia*. **238**: 71–78.

Longhurst, A., S. Sathyendranath, T. Platt & C. M. Caverhill 1995. An estimate of global primary production in the ocean from satellite radiometer data. *J. Plankton Res.* **17**: 1245–1271.

Lévy, M., L. Memery & G. Madec 1998. The onset of a bloom after deep winter convection in the north western Mediterranean Sea: Mesoscale process study with a primitive equation model. *J. Marine Syst.* **16**: 7–21.

Moisan, T. A. & B. G. Mitchell 1999. Photophysiological acclimation of *Pheocystis antarctica* Karsten under light limitation. *Limnol. Oceanogr.* **44**: 247–258.

Morel, A. & A. Bricaud 1981. Theoretical results concerning light absorption in a discrete medium, and application to specific absorption of phytoplankton. *Deep-Sea Res.* **28**: 1375–1393.

Ohi, N., Y. Ishiwata & S. Taguchi 2002. Diel patterns in light absorption and absorption efficiency factors of *Isochrysis galbana* (Prymnesiophyceae). *J. Phycol.* **38**: 730–737.

Sarmiento, J. L., R. D. Slater, M. J. R. Fasham, H. W. Ducklow, J. R. Toggweiler & G. T. Evans 1993. A seasonal three-dimensional ecosystem model of nitrogen cycling in the North Atlantic euphotic zone. *Global Biogeochem. Cycles* **7**: 417–450.

Siegel, D. A., T. D. Dickey, L. Washburn, M. K. Hamilton & B. G.

Mitchell 1989. Optical determination of particulate abundance and production variations in the oligotrophic ocean. *Deep-Sea Res.* **36**: 211–222.

Sosik, H. M. & B. G. Mitchell 1991. Absorption, fluorescence, and quantum yield for growth in nitrogen-limited *Dunaliella tertiolecta*. *Limnol. Oceanogr.* **36**: 910–921.

Sosik, H. M. & B. G. Mitchell 1994. The effects of temperature on growth, light absorption and quantum yield in *Dunaliella tertiolecta* (Chlorophyceae). *J. Phycol.* **30**: 833–840.

Stramska, M. & T. D. Dickey 1992. Variability of bio-optical properties of the upper ocean associated with diel cycles in phytoplankton populations. *J. Geophys. Res.* **97**: 17873–17887.

Stramski, D., A. Shalapyorok & R. A. Reynolds 1995. Optical characterization of the oceanic unicellular cyanobacterium *Synechococcus* grown under a day-night cycle in natural irradiance. *J. Geophys. Res.* **100**: 13295–13307.

Stramski, D. & R. A. Reynolds 1993. Diel variations in the optical properties of a marine diatom. *Limnol. Oceanogr.* **38**: 1347–1364.

van de Hulst, H. C. 1957. Light scattering by small particles. John Wiley. New York.

Zapata, M. & J. L. Garrido 1997. Occurrence of phytylated chlorophyll *c* in *Isochrysis galbana* and *Isochrysis* sp. (clone T-ISO) (Prymnesiophyceae). *J. Phycol.* **33**: 209–214.